

# Evaluating total outward leakage of face-worn products across various particle sizes for source control against submicron aerosols: Implications for public health protection

Weihua Yang<sup>a,\*</sup>, Warren R. Myers<sup>a</sup>, Kenneth J. Ryan<sup>b</sup>

<sup>a</sup> Department of Industrial and Management Systems Engineering, Statler College of Engineering and Mineral Resources, West Virginia University, Morgantown, WV 26506, USA

<sup>b</sup> Department of Statistics, West Virginia University, Morgantown, WV 26506, USA

## ARTICLE INFO

### Keywords:

ASTM  
Airborne transmission  
HEPA filter  
PM 2.5 filter  
Reusable masks  
Respiratory protection

## ABSTRACT

During COVID-19, the general public widely used face-worn products (FwPs) to mitigate viruses spread via airborne transmission. This study investigated the effectiveness of various FwP categories in reducing submicron aerosol transmission by evaluating total outward leakage (TOL) across particle sizes. Nine FwP categories were tested: ASTM F2100 Levels 1, 2, and 3 masks (categories 1–3); single-layer cloth mask (category 4); cloth masks with pockets, tested with and without HEPA and PM 2.5 filters insert (categories 5–8); and three-layer disposable masks (category 9). The TOL of these FwPs was assessed over multiple donnings on medium and large artificial headforms, and TOL mean diameter (TOLMD) was calculated. Results showed that cloth FwPs (categories 4–8) had higher TOL and a steeper increase with particle size (20–210 nm) compared to ASTM-compliant FwPs (categories 1–3) and disposable masks (category 9). Categories 4, 6, and 7 exhibited TOL values up to 60 % for particles >100 nm, which are significant for viral transmission. Non-ASTM-compliant products exhibited higher TOL for larger submicron particles. The analysis of TOLMD suggested that multiple donnings impact TOL across particle sizes. The findings established a link between TOL and particle size, providing more detailed guidance for the public in selecting FwPs for source control. This study also highlighted the importance of further research into the reusability of FwPs to inform public health recommendations for respiratory protection.

## 1. Introduction

During the COVID-19 pandemic, face-worn products (FwP), such as disposable masks and cloth masks, became essential for the general public because of their accessibility and reusability amidst a shortage of surgical masks and N95 respirators. While N95 respirators and surgical masks were prioritized for healthcare professionals, the public increasingly relied on disposable and cloth masks for source control (CDC, 2024; Cheng et al., 2021; Fennelly, 2020; Saunders et al., 2021).

Source control refers to the face covering's ability to capture and retain particles exhaled from the wearer's respiratory system so to help prevent the airborne transmission of exhaled particles from infected individuals who may or may not have symptoms of a specific respiratory disease (ASTM, 2020). Source control can be impacted by several factors: particle penetration through the filter material,

\* Corresponding author. 1306 Evansdale Dr, Morgantown, WV 26506, USA,  
E-mail address: [wy00002@mix.wvu.edu](mailto:wy00002@mix.wvu.edu) (W. Yang).

faceseal leakage, and, in some designs, exhalation valve emissions. For a comprehensive evaluation, total outward leakage (TOL) serves as a measure of overall particle escape from FwP during use (Myers et al., 2023).

Particle size is crucial in determining filtration efficiency, as smaller aerosols are more likely to penetrate. Studies have demonstrated variability in FwP performance based on particle size and mask material. For instance, Teising et al. (2020) measured the filtration efficiency of 25 materials at five particle sizes (0.3  $\mu\text{m}$ , 0.5  $\mu\text{m}$ , 1.0  $\mu\text{m}$ , 3.0  $\mu\text{m}$ , and 5.0  $\mu\text{m}$ ). They found the lowest efficiency (5 %–90 %) at 0.3  $\mu\text{m}$ , increasing to 36 %–100 % at 5  $\mu\text{m}$ , depending on the material. Additionally, Konda et al. (2020) found similar trends, with cloth-based FwP filtering 9 %–96 % of aerosols under 300 nm and 14 %–99.5 % for larger aerosols, depending on the fabric's properties.

Further research shows that N95 FFRs and cloth masks have higher filtration efficiency for larger particles ( $>1 \mu\text{m}$ ) compared to smaller ones ( $<1 \mu\text{m}$ ) (Hao et al., 2020; Rengasamy et al., 2010; Shakya et al., 2017; Zangmeister et al., 2020). Drewnick et al. (2021) reported the lowest efficiency in the 50–500 nm range, while Joshi et al. (2022) noted low efficiency at 60–140 nm for common disposable and cloth masks.

Recognizing faceseal leakage's impact on TOL is essential for a complete assessment of FwP in source control applications. Current standards such as ASTM F2100 and F3502 guide the testing of medical masks and barrier face coverings but do not fully account for faceseal or exhalation valve leakage effects (ASTM, 2020, 2023). When an FwP is sealed on a test headform, particle penetration through the filter material is the primary source of leakage. However, achieving a complete fit is rarely possible, as faceseal gaps are common and significantly impact both wearer protection and source control (Drewnick et al., 2021; Joshi et al., 2022; Konda et al., 2020; Rengasamy et al., 2010). Relying solely on filtration efficiency to assess source control, therefore, is insufficient.

Regarding the faceseal gap, some studies have correlated particle size with source control, demonstrating that FwP tends to be more effective as particle size increases. Research shows that mask use reduces the size of exhaled particles compared to unmasked conditions during activities like coughing, and collection efficiency for homemade cloth masks rises with particle size (Asadi et al., 2020; Lindsley et al., 2021).

Understanding how TOL varies with particle size is crucial for assessing the impact of FwPs on aerosol transmission, as particle size significantly influences airborne behavior and transmission dynamics (Pöhlker et al., 2021; Prather et al., 2020; Samet et al., 2021; Wang et al., 2021). This present study builds on our previous work, which examined the overall TOL, irrespective of particle size, for various FwPs commonly used by the general public for source control (Yang et al., 2025a). Unlike that study, the current work specifically investigates how TOL varies with particle size, offering a detailed analysis of particle-size-dependent leakage patterns across a range of submicron particles. Additionally, a prior study on the TOL of surgical masks and half-mask respirators for healthcare workers across different particle sizes provided a robust methodology for analyzing TOL as a function of particle size (Yang et al., 2025b).

Expanding on these foundations, the present study evaluates the impacts of factors such as FwP category, facial size, and multiple donning on TOL across particle sizes. The TOL mean diameter (TOLMD), calculated as the mean of particle sizes weighted by TOL at each particle size bin, elucidates how outward leakage behaves across the size spectrum under different conditions. By addressing the interplay between particle size and key influencing factors, this study provides a more comprehensive understanding of the TOL of commonly used FwPs for source control.

## 2. Methods

### 2.1. Test face-worn products

Nine categories of FwPs were tested, with two models randomly selected per category. Category 1, 2, and 3 FwPs were compliant, respectively, with ASTM F2100 Level 1, 2, and 3 test criteria. Categories 4–8 were all cloth FwPs. Category 4 FwP were single-layer cloth masks. Category 5 FwPs were cloth masks equipped with a pocket (CMPs) for using a high-efficiency particulate air (HEPA) filter

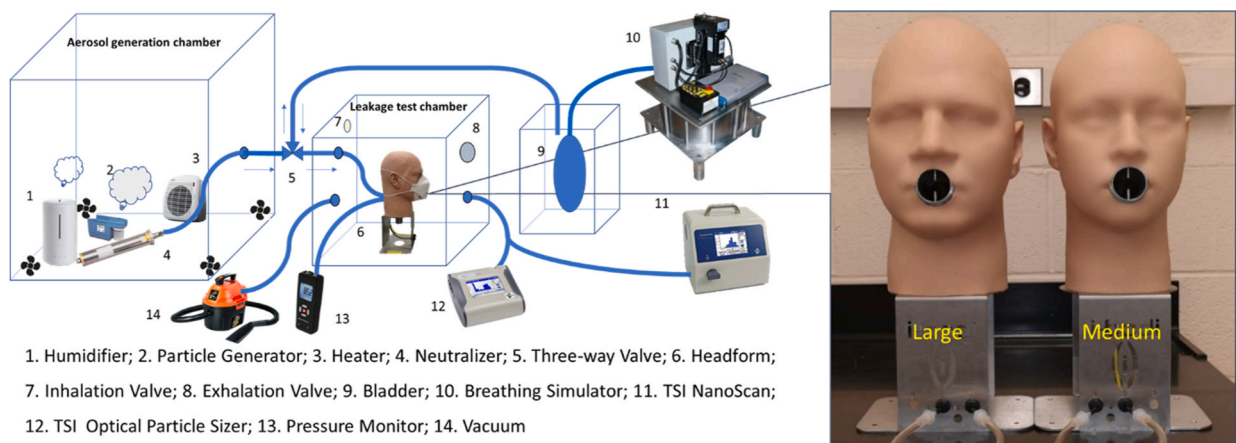


Fig. 1. The TOL test system and headforms with artificial skin surface (Yang et al., 2025a).

tested without the insert, and Category 6 FwPs were the same as Category 5 FwPs but tested with the HEPA insert in place. Category 7 FwPs were CMPs for using a particulate matter (PM) 2.5 filter tested without the insert. Category 8 FwPs were the same as Category 7 FwPs but tested with the PM 2.5 filter insert in place. Category 9 FwPs were three-layer disposable masks. All masks used ear loops, lacked exhalation valves, and were tested over five donnings to simulate reuse. The images of the tested FwPs are provided in [Table S1](#) of the Supplementary Information, and the pictures of filters inserted into the CMPs are shown in [Fig. S1](#) of the Supplementary Information. Additionally, [Fig. S2](#) of the Supplementary Information illustrates how the filters are inserted into the CMPs.

## 2.2. Test setup

The experimental setup for measuring the TOL<sub>i</sub> at different particle sizes is shown in [Fig. 1](#) and was identical to that described in detail in a previous study ([Yang et al., 2025a](#)). The system includes two testing chambers: the aerosol generation chamber (1.73 m<sup>3</sup>: 1.2 m × 1.2 m × 1.2 m) and leakage testing chamber (0.26 m<sup>3</sup>: 0.75 m × 0.59 m × 0.59 m). In the aerosol generation chamber, the aerosol was generated using a particle generator (Model 8026; TSI, Inc., Shoreview, MN) with the NaCl solution with a concentration of 2 %. The aerosol generation chamber was controlled with temperature and humidity maintained at 32 ± 2 °C and 60 ± 2 %, respectively. An aerosol neutralizer (Model 3054, TSI Inc., Shoreview, MN, USA) was employed to achieve Boltzmann charge equilibrium for the NaCl aerosol before exhaling to the headform. In the leakage testing chamber, two headforms with medium and large face sizes of the U.S. civilian worker population ([Zhuang et al., 2007](#)) were employed to mount the FwPs. Additionally, these advanced headforms had a compressible silicone elastomer skin to simulate the interface between the FwPs and a user's face close to reality.

When testing the TOL of a FwP, the aerosols in the aerosol generation chamber were drawn by a dynamic breathing machine (Warwick Technology Limited, Warwick, UK) to the headform wearing a FwP in the leakage testing chamber. The breathing machine simulated human breathing following a half-sinusoid flow rate. A three-way check valve connected the particle generation chamber, the headform in the leakage test chamber, and the breathing machine, preventing aerosol re-inhalation through the FwPs. A sinusoidal breathing pattern at a minute ventilation flowrate of 28 L/min (25 BPM × 1.12 L/breath) was used to simulate the breathing of the general public doing moderate work rate activities. The minute ventilation flowrate was calculated according to "ISO/TS 16976-1; Respiratory protective devices - Human factors - Part 1: Metabolic rates and respiratory flowrates" ([International Organization for Standardization, 2015](#)).

A NanoScan SMPS (Model 3910, TSI Inc., Shoreview, MN, USA) and an Optical Particle Sizer (Model 3330, TSI Inc., Shoreview, MN, USA) were used to measure aerosol number concentrations and particle size distributions. Although the OPS was connected throughout the testing, its data (measuring particles >300 nm) was not included in this study due to low particle concentrations in that size range under our experimental conditions, rendering the data statistically unreliable. Both devices were sent back to the manufacturer annually for calibration on the recommended date.

## 2.3. Test procedure

At the beginning of each test, the FwP was fitted on the headform and adjusted while monitoring the real-time manikin fit factor (MFF), shown as [Table S2](#) of Supplementary Information, in the aerosol chamber using a PortaCount Pro + Respirator Fit Tester (model 8038, TSI Inc., MN, USA). MFF refers to manikin fit factor, calculated as the ratio of outside to inside particle concentration averaged over the particle size range. A higher MFF indicates a better faceseal performance (i.e., lower inward leakage). The real-time MFF tracked how the fit of the FwP changed with its position on the headform. The headform with the FwP was then moved to the test chamber once the MFF stabilized at its maximum possible value.

Next, the number concentration of upstream aerosol was measured inside the cavity of the FwP, and the number concentration of downstream aerosol was measured outside the mask in the leakage testing chamber. Before each test, the leakage testing chamber was flushed with fresh air to maintain a low background aerosol number concentration. The background aerosol concentration values, listed in [Table S3](#), averaged 35 particles/cm<sup>3</sup> (±1.6) across all tests. The upstream aerosol number concentration had a mean of 100,132 particles/cm<sup>3</sup> (±2378), and the downstream aerosol had a mean of 35,184 particles/cm<sup>3</sup> (±1236). The upstream aerosol exhibited a count median diameter (CMD) of approximately 0.113 μm and a geometric standard deviation (GSD) of 1.72, while the particle size characteristics of the downstream aerosol varied depending on the FwP used.

Upstream and downstream aerosol number concentrations were recorded across 29 particle size bins ranging from 11 nm to 8962 nm using NanoScan and OPS. However, data points for these particle size bins of 11 nm, 15 nm, and larger than 210 nm were excluded due to the low number concentrations detected and the inaccuracy of NanoScan for these particle sizes due to its unipolar charging process ([Fonseca et al., 2016](#)). Finally, TOL<sub>i</sub> at each particle bin from 20 nm to 210 nm was calculated by subtracting the test chamber's background aerosol number concentration from the downstream aerosol number concentration leaking through the filter and faceseal, divided by the upstream aerosol number concentration. Calculations for each particle size bin followed Equation (1), consistent with our previous study ([Yang et al., 2025b](#)).

$$TOL_i = (C_{outi} - C_{bgi}) / C_{ini} \quad (1)$$

where.

$TOL_i$  = TOL of FwPs for particles in group  $i$  having a midpoint size  $D_p$

$C_{ini}$  = Number concentration inside the FwP's cavity for particles in group  $i$  having a midpoint size  $D_p$

$C_{bgi}$  = Number concentration of background in the test chamber for particles in group  $i$  having a midpoint size  $D_p$

$C_{outi}$  = Number concentration outside the FwP's cavity in the test chamber for particles in group  $i$  having a midpoint size  $D_p$

The TOLMD was used to measure the particle size characteristic of the TOL. The TOLMD and standard deviation (SD) were calculated using Equation 2.a and 2.b, respectively:

$$TOLMD = \frac{\sum (D_p \times TOL_i)}{\sum TOL_i} \quad (2. a)$$

$$SD = \frac{\sum ((D_p - TOLMD) \times TOL_i)}{\sum TOL_i} \quad (2. b)$$

where.

$D_p$  = midpoint particle size

$TOL_i$  = TOL of particles in group  $i$  having a midpoint size  $D_p$ .

#### 2.4. Experimental design and data analysis

The experiment design in this study utilized a three-factor full factorial design approach to investigate the impact of FwP category, headform size, and donning on the TOLMD for each FwP (Montgomery, 2017). The linear statistical model for this factorial design is:

$$Y_{ijkl} = \mu + \tau_i + \beta_j + \gamma_k + (\tau\beta)_{ij} + (\beta\gamma)_{jk} + (\tau\gamma)_{ik} + (\beta\gamma\delta)_{ijk} + \epsilon_{ijkl} \quad \begin{cases} i = 1, 2, 3, 4, 5, 6, 7, 8, 9 \\ j = 1, 2 \\ k = 1, 2, 3, 4, 5 \\ l = 1, 2 \end{cases} \quad (3)$$

where  $\mu$  is the overall mean effect,  $\tau_i$  represents the effect of the  $i$  th level of the FwP category,  $\beta_j$  represents the effect of the  $j$  th level of headform,  $\gamma_k$  represents the effect of  $k$  th donning,  $(\tau\beta)_{ij}$  represents the effect of the interaction between  $\tau_i$  and  $\beta_j$ ,  $(\tau\gamma)_{ik}$  represents the

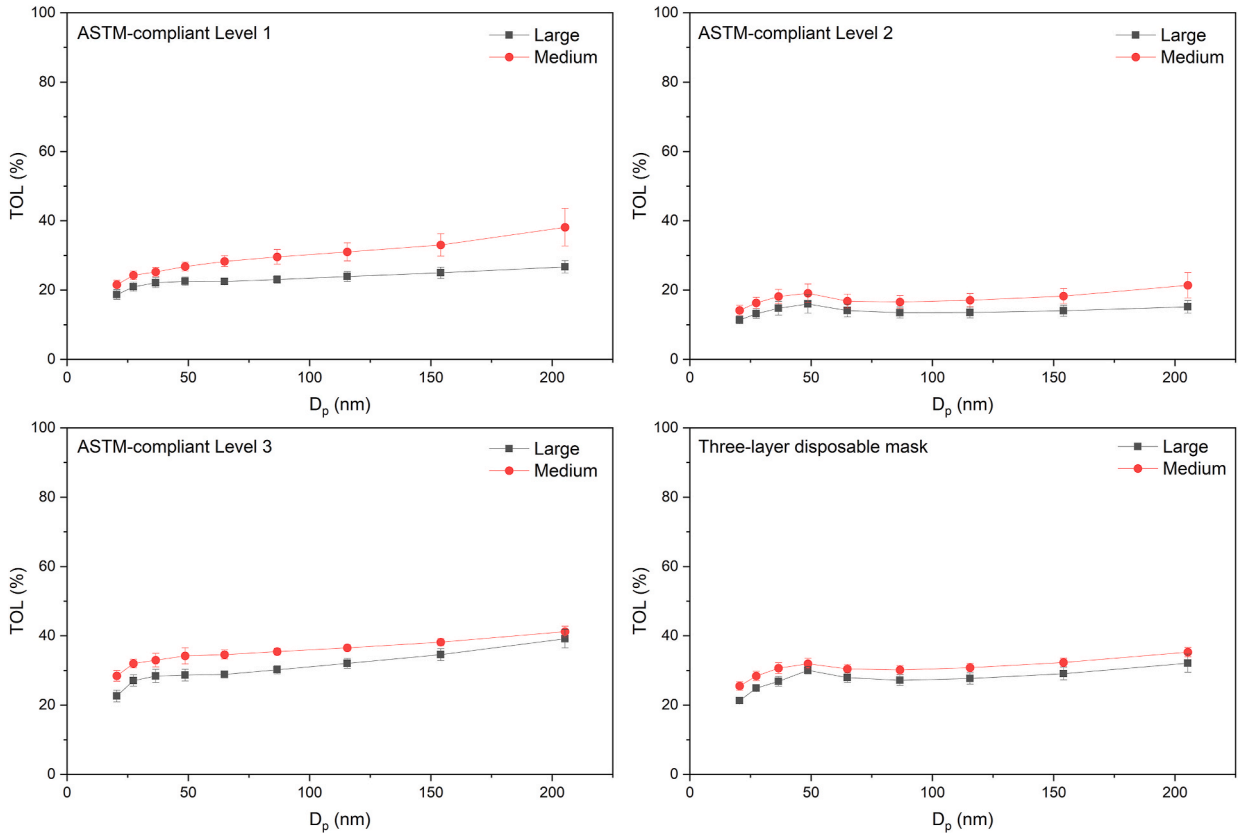


**Fig. 2.** TOL of ASTM F2100-compliant face masks and three-layer disposable masks across particle sizes from 20 to 210 nm. The TOL value is averaged across five donnings, each error bar is constructed using 1 standard error from the mean.

effect of the interaction between  $\tau_i$  and  $\gamma_k$ ,  $(\beta\gamma)_{jk}$  represents the effect of the interaction between  $\beta_j$  and  $\gamma_k$ ,  $(\tau\beta\gamma)_{ijk}$  represents the effect of interaction among  $\tau_i$ ,  $\beta_j$  and  $\gamma_k$ , and  $\varepsilon_{ijkl}$  is a random error component.

A total of 180 observations were performed in the study, with each of the nine FwPs undergoing five donnings on two different headform sizes (nine FwPs categories  $\times$  two devices per category  $\times$  two headform sizes  $\times$  five donnings). The TOL values are averaged across 10 observations for each FWP category (two FwPs/category  $\times$  five donnings per FWP). The test sequence of each observation was randomized. The group data were compared using a three-way analysis of variance (ANOVA) with the significance level of  $\alpha = 0.05$ . The statistical analysis was conducted using JMP software (Sall et al., 2017).

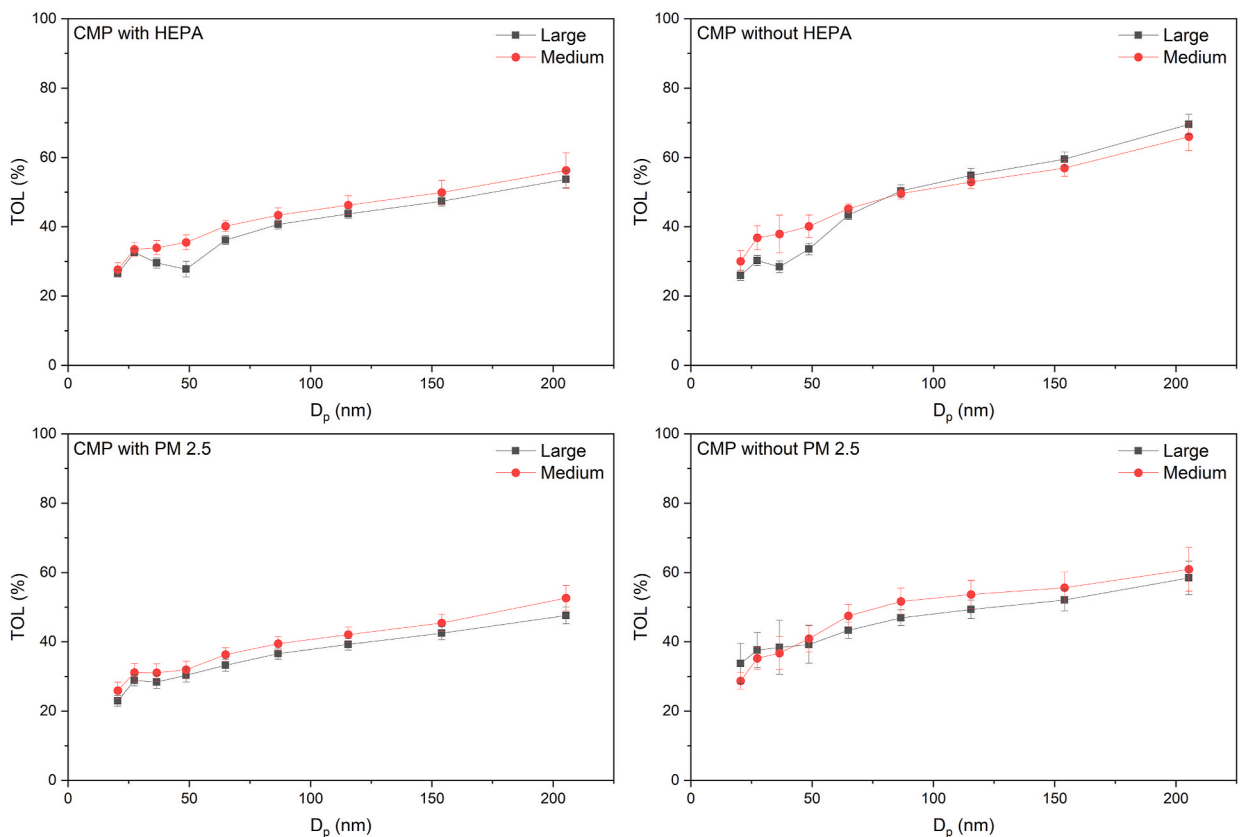
### 3. Results

Fig. 2 shows the TOL of ASTM F2100 compliant FwPs (categories 1, 2, and 3), as well as three-layer disposable masks (category 9), across a particle size range of 20–210 nm on medium and large headforms. These four FWP categories exhibited TOLs from  $\sim 15\%$  to  $\sim 40\%$  across this range. Categories 1, 2, and 3 demonstrated consistent TOL values across both headform sizes throughout the 20–210 nm particle size range. FWP categories in Fig. 2 showed slight TOL increases with particle size. ASTM F2100-compliant level 2 FWP and three-layer disposable FWP (categories 2 and 9) demonstrated similar TOL trends, exhibiting a convex pattern from 20 nm to 90 nm, followed by a continued increase. The TOL of the three-layer disposable mask on both headforms also reflected these trends.

Fig. 3 illustrates the TOLs for CMPs with or without filter insert (categories 5, 6, 7, and 8). These cloth FwPs are equipped with pockets so they can be used with or without a HEPA or PM 2.5 filter insert. For CMPs with a HEPA filter insert (category 6), TOL increased from 25 % to 55 % as particle size rose from 20 to 210 nm, whereas without the HEPA filter insert (category 5), TOL was higher, ranging from 25 % to 70 %. CMPs with and without a PM 2.5 filter insert (categories 8 and 7) similarly showed rising TOLs with particle size: with the insert, TOL increased from 25 % to 52 %; without it, TOL ranged from 29 % to 61 %. Fig. 4 shows the TOLs of single-layer cloth masks. Again, the TOL of the single-layer cloth masks increased with particle size.

Table 1 presents the ANOVA analysis on the TOLMD as a function of FWP category, headform, donning, and interactions. The ANOVA found that only the FWP category (P-Value  $< 0.0001$ ) and donnings (P-Value = 0.0480) had significant effects on the TOLMD. To provide additional context, TOL values corresponding to each condition are included alongside TOLMD in Table S5 of the Supplementary Information.

Further paired comparison analysis by category and donning using Student's t-test was conducted. Table 3 lists the mean of TOLMD



**Fig. 3.** TOL of CMPs for HEPA with and without filter insert and CMPs for PM 2.5 with and without filter insert across particle sizes. The TOL value is averaged across five donnings, each error bar is constructed using 1 standard error from the mean.



for each independent variable, with significant differences indicated by superscript letters. For example, TOLMD for categories 4, 5, 6, 7, and 8 FwPs was significantly higher than for categories 1, 2, 3, and 9. The single-layer cloth mask (category 4) had a TOLMD of 94.2 nm, significantly greater than 87.1 nm for the three-layer disposable mask (category 9) and 88.8 nm for the ASTM F2100 level 2 mask (category 2). TOLMD for CMPs with or without HEPA and PM 2.5 filter inserts (categories 5 and 7) ranged from 96.3 to 101.0 nm, with no significant differences. The mean TOLMD for ASTM F2100 level 1, level 2, and level 3 compliant masks (categories 1, 2, and 3) and the three-layer disposable masks (category 9) ranged from 87.1 to 91.5 nm, also showing no significant differences.

Table 2 displays the TOLMD of various FwPs at each donning, with the results of Student's t-test presented as superscript letters behind the mean values. The data suggested that the first donning resulted in a larger TOLMD of 97.8 nm compared to subsequent donnings, which exhibited identical TOLMD values ranging from 92.3 to 93.1 nm. Further paired comparison between each combination of FwP category and donning revealed that the ASTM-compliant Level 1, Level 2, and Level 3 masks had significantly higher TOLMD values during the first donning compared to later donnings while other FwPs did not show significant difference in TOLMD among donnings (see Table S5 in Supplementary Information).

Fig. 5 presents the TOL of ASTM-compliant Level 1, Level 2, and Level 3 masks across particle sizes at different donnings. At the first donning, Level 1 and Level 2 masks exhibited the lowest TOL for particles  $< \sim 70$  nm and the highest TOL for particles  $> \sim 100$  nm. The Level 3 mask showed the lowest TOL at first donning for particles  $< \sim 70$  nm and comparable TOL to subsequent donnings for larger particles. This phenomenon resulted in the larger TOLMD at first donning compared to subsequent donnings. This pattern contributed to the higher TOLMD observed at the first donning compared to later ones.

#### 4. Discussion

In this study, we evaluated the TOL of various FwPs used by the general public, with particular attention to how TOL varies across submicron particle sizes. While our previous research focused on the overall TOL without taking particle size into account and addressed factors such as FwP category, headform size, and multiple donning (Yang et al., 2025a), this study specifically explores the particle-size dependence of TOL. To our knowledge, this is the first study to examine a broad spectrum of commonly used FwPs in the context of TOL across different particle sizes.

A key innovation in this study is the introduction of the TOLMD that provides a clearer understanding of how leakage varies across the size spectrum. By reflecting the particle sizes weighted by TOL, TOLMD enables a more nuanced understanding of leakage trends that would be overlooked by traditional evaluations. Unlike conventional evaluations that focus solely on filtering material, this study incorporates the impact of face seal leakage, considering factors such as facial size and multiple donning. This integrative approach presents a more comprehensive evaluation of FwP effectiveness in mitigating aerosol transmission.

Our findings show that TOL for all FwPs increased with particle size across the 21–210 nm range. Cloth FwPs, including single-layer cloth masks and CMPs with and without filter insert (categories 4–8), exhibited a rapid TOL increase as particle size grew, while ASTM F2100-compliant FwPs and three-layer disposable masks (categories 1–3 and 9) showed a slower TOL rise. This increasing trend likely results from different filtration mechanisms: for particles smaller than 200 nm, diffusion plays a dominant role, reducing filtration efficiency as size increases (Tcharkhtchi et al., 2021). Additionally, larger aerosols experience air as a continuum rather than as individual particles, resulting in greater drag forces as they move through the air (James H., 1995). This increased drag may enable them to deviate more readily from the airstream when encountering face seal gaps, thereby increasing their likelihood of escaping.

While our study observed that the TOL of FwPs increased with particle size for particles smaller than 210 nm, aerosol collection efficiency (i.e.,  $1 - \text{TOL}$ ) showed a corresponding decrease in TOL for particles larger than 600 nm (Lindsley et al., 2021). This trend was particularly evident for homemade cloth masks. Zangmeister et al. (2020) reported that the filtration efficiency of surgical and cloth masks decreased with particle size from 5 nm to 200 nm, with the highest particle penetration occurring around 200–300 nm. However, their study evaluated only filtration efficiency and did not account for face seal leakage. Face seal gaps, which may enlarge during exhalation, can allow larger particles to bypass the filter and contribute to outward leakage—an effect not captured by filtration

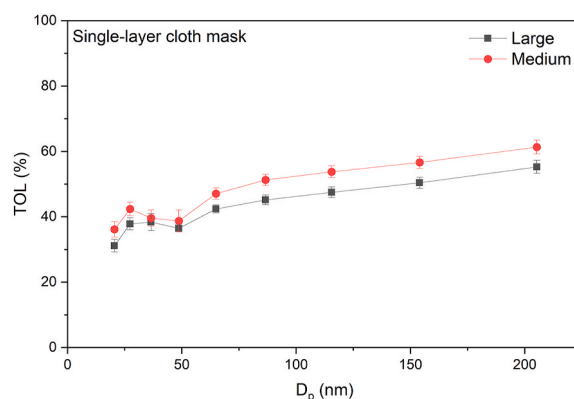


Fig. 4. TOL of single-layer cloth masks across particle sizes. The TOL value is averaged across five donnings, each error bar is constructed using 1 standard error from the mean.

**Table 1**

ANOVA results of TOLMD by category, headform size, donning and their interactions.

Source	DF	SS	MS	F	P-Value
Category	8	3226.6	403.3	5.6	<0.0001*
Headform Size	1	8.5	8.5	0.1	0.7322
Category*Headform Size	8	265.6	33.2	0.5	0.8800
Donning	4	719.1	179.8	2.5	0.0480*
Category*Donning	32	1580.2	49.4	0.7	0.8849
Headform Size* Donning	4	501.2	125.3	1.7	0.1477
Category*Headform Size* Donning	32	1366.2	42.7	0.6	0.9515

Note: “\*” behind the P-Values means there is a significant effect; “DF” means the degrees of freedom in the source; “SS” means the sum of squares due to the source; “MS” means the mean sum of squares due to the source; “F” means F-statistic.

**Table 2**

Student's t-test analysis for mean TOLMD by category of FwP.

FwP category	n	Mean	Std Dev	Lower 95 %	Upper 95 %
Cat-5 CMP for HEPA without filter	20	101.0 <sup>A</sup>	8.8	96.9	105.1
Cat-8 CMP for PM 2.5 with filter	20	97.2 <sup>AB</sup>	5.0	94.8	99.6
Cat-6 CMP for HEPA with filter	20	97.1 <sup>AB</sup>	6.5	94.1	100.1
Cat 7 CMP for PM 2.5 without filter	20	96.3 <sup>ABC</sup>	14.2	89.7	103.0
Cat 4 cloth single-layer mask	20	94.2 <sup>BC</sup>	4.8	92.0	96.5
Cat-3 ASTM F2100-compliant Level3	20	91.5 <sup>CD</sup>	6.4	88.5	94.5
Cat-1 ASTM F2100-compliant Level1	20	91.2 <sup>CD</sup>	8.7	87.1	95.2
Cat-9 Three-layer disposable mask	20	88.8 <sup>D</sup>	4.5	86.7	91.0
Cat-2 ASTM F2100-compliant Level2	20	87.1 <sup>D</sup>	8.2	83.3	91.0

Note: FwP categories connected by different superscript letters are significantly different.

**Table 3**

TOLMD of various face-worn products for different donnings.

Donning	Mean	Std Dev	Lower 95 %	Upper 95 %
Donning 1	97.8 <sup>A</sup>	9.6	94.6	101.0
Donning 2	93.0 <sup>B</sup>	9.5	89.8	96.2
Donning 3	92.9 <sup>B</sup>	7.8	90.3	95.6
Donning 4	93.1 <sup>B</sup>	9.1	90.1	96.2
Donning 5	92.3 <sup>B</sup>	7.6	89.8	94.9

Note: Donnings connected by different superscript letters are significantly different.

efficiency measurements alone. This discrepancy between filtration-based studies and real-world leakage measurements highlights the need to evaluate TOL as a function of particle size while considering faceseal gaps, particularly within the 210–600 nm range. The observed gap in TOL behavior within this particle size range, as seen in both our study and [Lindsley et al. \(2021\)](#), warrants further investigation to identify the particle size associated with the highest outward leakage.

Cloth FwPs (categories 4–8) demonstrated higher TOL across particle sizes. Additionally, the analysis of TOLMD revealed that larger particles are influential to the TOL of these FwPs. This is reasonable because FwPs with filtering material of cloth are less effective at capturing larger aerosols compared to non-woven materials, resulting in the shift of TOL towards larger particle sizes for cloth FwPs ([Konda et al., 2020](#)). Consequently, we observed a high TOL of cloth FwPs. TOL exceeding 60 % for aerosols >100 nm with these categories of FwP are particularly important because they are of a size likely to carry viruses such as SARS-CoV-2 ([Pöhlker et al., 2021](#)).

It is important to highlight that the TOL of an ASTM-compliant level 2 mask and a three-layer disposable mask exhibited a convex trend for particles sized between 20 nm and 90 nm, a pattern distinct from other FwPs. A likely explanation for this trend is that these two types of face masks achieved a relatively better fit according to MFF ([Table S2](#) of Supplementary Information), leading to a larger proportion of particles being filtered through the mask material rather than escaping through the faceseal gap. However, the filtration efficiency in this size range was reduced due to the combined effects of diffusion and interception mechanisms, which are less effective for particles in this size range ([Tcharkhtchi et al., 2021](#); [Todea et al., 2020](#)).

Another noteworthy pattern is the drop in TOL observed around 35 nm–50 nm for CMPs, with and without filter insert, and single-layer cloth masks. It may be due to the poor fit of these cloth FwPs on the headform. As a result, a more proportion of particles likely escaped through the faceseal gap and interacted with the headform surface ([Dahneke, 1971](#)). A similar phenomenon was observed in our previous study on surgical masks and N95 FFRs when they were not fully sealed on the headform ([Yang et al., 2025b](#)). The interaction between the exhaled aerosols and the faceseal surface needs further study. Another possible reason could be the over-estimation of particle number concentrations smaller than 60 nm by the NanoScan, as reported by [Fonseca et al. \(2016\)](#).

It's important to acknowledge that multiple donnings have a notable effect on TOLMD. The initial donning was found to have the

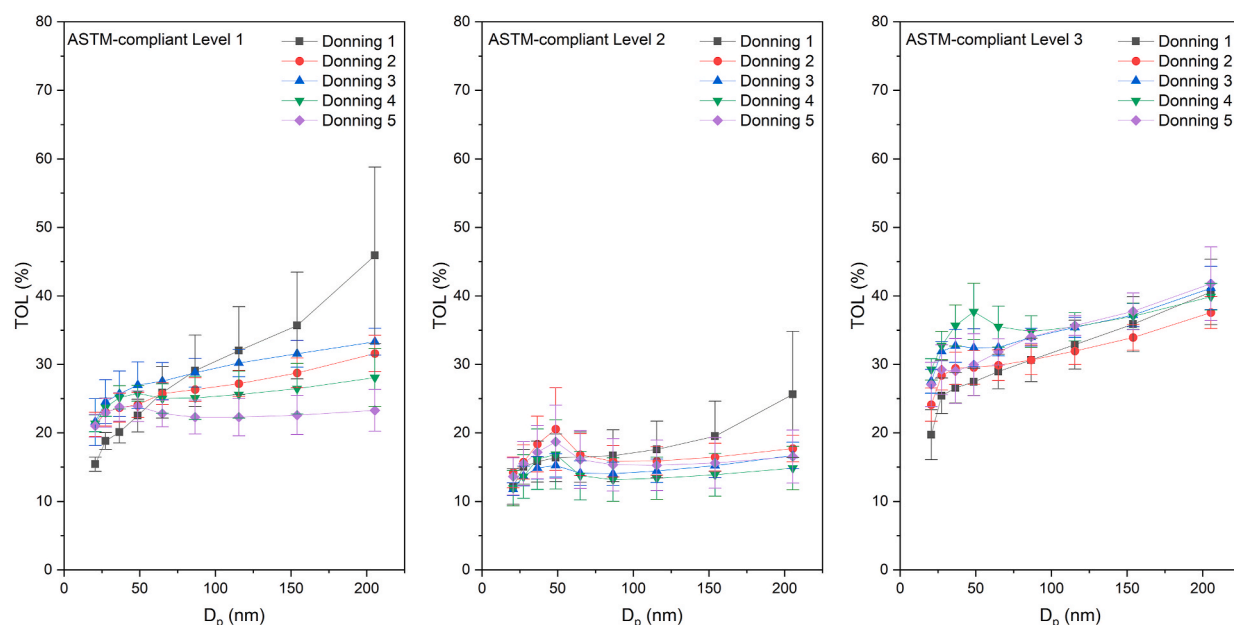


**Fig. 5.** The TOL of the ASTM-compliant masks across particle sizes at different donnings. The TOL value is averaged across two mask models on two sized headforms, and each error bar is constructed using 1 standard error from the mean.

highest TOLMD, with subsequent donnings showing no significant differences. This phenomenon may stem from the fit of the face-covering, which is influenced by multiple donnings. To date, there hasn't been a study specifically examining the impact of multiple donnings of commonly used FwPs on TOL. However, insights can be drawn from studies on N95 respirators. Bergman et al. (2012) observed that the percentage of fit factors for N95 respirators  $>100$  decreased with multiple donnings (Bergman et al., 2012). Another possible explanation could be the loading of aerosols on the filtering materials. A study has indicated that loading time decreased the most penetrating particle size (MPPS) for N95 FFRs, which corroborated our findings (Mahdavi, 2013).

When examining the impact of donning on the TOL of ASTM-compliant masks across particle sizes, larger particles ( $>100$  nm) were more likely to leak during the first donning, while smaller particles ( $<70$  nm) were more likely to leak in subsequent donnings. One possible explanation is that during the first donning, the nose wire may not bend sufficiently to ensure a proper fit, resulting in increased leakage of larger particles. In contrast, improved fit during later donnings may reduce facesal leakage of larger particles, but previously deposited particles on the filter fibers could reduce capture efficiency for smaller particles. Nevertheless, the effects of multiple donnings and particle loading on TOL across particle sizes warrant further investigation in future studies.

This study has several limitations that should be considered. First, it focused exclusively on submicron aerosols, potentially limiting its applicability to larger aerosols that are more likely to carry viruses. Future research should address both submicron and larger aerosols, particularly the particle size gap between 210 nm and 600 nm (Lindsley et al., 2021), to better understand the broader impact of FwPs on aerosol transmission. Second, while particle number concentration was used to calculate TOL in this study, incorporating mass concentration measures would provide a more robust and comprehensive evaluation. Third, inaccuracies in NanoScan measurements for certain particle size ranges in particle number concentration may have introduced errors in the TOL outcomes, even though data points for these bins were excluded and TOL was calculated as a relative ratio.

Additionally, this study primarily assessed TOL by simulating real-world usage of FwPs, rather than focusing solely on filtration efficiency. While this approach offers valuable insights into outward leakage, future research should also examine filtration efficiency to gain a more detailed understanding of how leakage occurs. The study also tested FwPs for only five donnings, which may not adequately capture the effects of repeated use on source control performance. Lastly, factors such as fabric category, thread count, and density, which can significantly influence FwP performance, were not strictly controlled. Addressing these limitations in future research will enhance our understanding of FwP effectiveness in mitigating aerosol transmission and contribute to more evidence-based public health recommendations.

## 5. Conclusions

In conclusion, our study provides valuable insights into the performance of FwPs in mitigating submicron aerosol transmission, particularly concerning TOL across various particle sizes from 20 nm to 210 nm. Our analysis revealed an increasing trend in TOL with larger particle sizes, underscoring the challenges posed by submicron particles, especially for aerosols  $>100$  nm that have the potential to carry viruses. Additionally, different categories of FwPs exhibited variations in TOL across particle sizes. ASTM F2100-compliant FwPs (categories 1–3) and three-layer disposable masks (category 9) consistently exhibited lower TOL across particle sizes than



cloth FwPs (categories 4–8), including single-layer cloth masks and CMPs whether with or without filter insert.

Notably, the cloth FwPs exhibited high a TOL of up to 60 % for aerosols >100 nm, raising concerns about their efficacy in viral particle containment. Furthermore, our study underscored the impacts of multiple donnings on TOLMD, indicating potential changes in particle size of TOL due to alterations in fit or aerosol loading when reusing these FwPs. This observation underscores the importance of considering the effects of repeated use on FwP effectiveness. Future research should address the impacts of multiple donnings and loading time on TOL particle size in greater detail.

### CRediT authorship contribution statement

**Weihua Yang:** Writing – review & editing, Writing – original draft, Visualization, Validation, Methodology, Investigation, Formal analysis, Data curation, Conceptualization. **Warren R. Myers:** Writing – review & editing, Supervision, Resources, Project administration, Funding acquisition, Conceptualization. **Kenneth J. Ryan:** Writing – review & editing, Validation, Data curation.

### Disclosure

During the preparation of this work the authors used ChatGPT in order to improve the grammar and language clarity. After using this tool, the authors reviewed and edited the content as needed and took full responsibility for the content of the publication.

### Funding

This study was funded by the National Institute for Occupational Safety and Health (NIOSH), National Personal Protective Technology Laboratory (NPPTL) (Contract # 75D30120P09521).

### Declaration of competing interest

The authors declare the following financial interests/personal relationships which may be considered as potential competing interests Warren R. Myers reports financial support was provided by National Institute for Occupational Safety and Health. If there are other authors, they declare that they have no known competing financial interests or personal relationships that could have appeared to influence the work reported in this paper.

### Acknowledgment

The authors would like to thank National Personal Protective Technology Laboratory staff members for their support in our work.

### Appendix A. Supplementary data

Supplementary data to this article can be found online at <https://doi.org/10.1016/j.jaerosci.2025.106586>.

### Data availability

No data was used for the research described in the article.

### References

- Asadi, S., Cappa, C. D., Barreda, S., Wexler, A. S., Bouvier, N. M., & Ristenpart, W. D. (2020). Efficacy of masks and face coverings in controlling outward aerosol particle emission from expiratory activities. *Scientific Reports*, 10(1), Article 15665. <https://doi.org/10.1038/s41598-020-72798-7>
- ASTM. (2020). *Specification for Performance of materials Used in medical face masks (versions F2100 – 20)*. ASTM International. <https://doi.org/10.1520/F2100-21>
- ASTM. (2023). *Specification for barrier face coverings (versions F3502 – 23)*. ASTM International. <https://doi.org/10.1520/F3502-23A>
- Bergman, M. S., Viscusi, D. J., Zhuang, Z., Palmiero, A. J., Powell, J. B., & Shaffer, R. E. (2012). Impact of multiple consecutive donnings on filtering facepiece respirator fit. *American Journal of Infection Control*, 40(4), 375–380. <https://doi.org/10.1016/j.ajic.2011.05.003>
- CDC. (2024). Interim infection prevention and control recommendations for healthcare personnel during the coronavirus disease 2019 (COVID-19) pandemic. <https://www.cdc.gov/coronavirus/2019-ncov/hcp/infection-control-recommendations.html>
- Cheng, Y., Ma, N., Witt, C., Rapp, S., Wild, P. S., Andreae, M. O., Pöschl, U., & Su, H. (2021). Face masks effectively limit the probability of SARS-CoV-2 transmission. *Science*, 372(6549), 1439–1443. <https://doi.org/10.1126/science.abg6296>
- Dahneke, B. (1971). The capture of aerosol particles by surfaces. *Journal of Colloid and Interface Science*, 37(2), 342–353. [https://doi.org/10.1016/0021-9797\(71\)90302-X](https://doi.org/10.1016/0021-9797(71)90302-X)
- Drewnick, F., Pikmann, J., Fachinger, F., Moormann, L., Sprang, F., & Borrmann, S. (2021). Aerosol filtration efficiency of household materials for homemade face masks: Influence of material properties, particle size, particle electrical charge, face velocity, and leaks. *Aerosol Science and Technology*, 55(1), 63–79. <https://doi.org/10.1080/02786826.2020.1817846>
- Fennelly, K. P. (2020). Particle sizes of infectious aerosols: Implications for infection control. *The Lancet Respiratory Medicine*, 8(9), 914–924. [https://doi.org/10.1016/S2213-2600\(20\)30323-4](https://doi.org/10.1016/S2213-2600(20)30323-4)

- Fonseca, A. S., Viana, M., Pérez, N., Alastuey, A., Querol, X., Kaminski, H., Todea, A. M., Monz, C., & Asbach, C. (2016). Intercomparison of a portable and two stationary mobility particle sizers for nanoscale aerosol measurements. *Aerosol Science and Technology*, 50(7), 653–668. <https://doi.org/10.1080/02786826.2016.1174329>
- Hao, W., Parasc, A., Williams, S., Li, J., Ma, H., Burken, J., & Wang, Y. (2020). Filtration performances of non-medical materials as candidates for manufacturing facemasks and respirators. *International Journal of Hygiene and Environmental Health*, 229, Article 113582. <https://doi.org/10.1016/j.ijheh.2020.113582>
- International Organization for Standardization. (2015). *Respiratory protective devices—human factors—Part 1: Metabolic rates and respiratory flow rates*. No. ISO/TS 16976-1).
- James, H. V. (1995). *Aerosol science for industrial hygienists* (1st ed.). Elsevier.
- Joshi, M., Khan, A., & Sapra, B. (2022). Quick laboratory methodology for determining the particle filtration efficiency of face masks/respirators in the wake of COVID-19 pandemic. *Journal of Industrial Textiles*, 51(5 suppl), 7622S–7640S. <https://doi.org/10.1177/1528083720975084>
- Konda, A., Prakash, A., Moss, G. A., Schmoldt, M., Grant, G. D., & Guha, S. (2020). Aerosol filtration efficiency of common fabrics used in respiratory cloth masks. *ACS Nano*, 14(5), 6339–6347. <https://doi.org/10.1021/acsnano.0c03252>
- Lindsley, W. G., Blachere, F. M., Law, B. F., Beezhold, D. H., & Noti, J. D. (2021). Efficacy of face masks, neck gaiters and face shields for reducing the expulsion of simulated cough-generated aerosols. *Aerosol Science and Technology*, 55(4), 449–457. <https://doi.org/10.1080/02786826.2020.1862409>
- Mahdavi, A. (2013). *Efficiency measurement of N95 filtering facepiece respirators against ultrafine particles under cyclic and constant flows*. Concordia University [Masters thesis]. <https://spectrum.library.concordia.ca/id/eprint/977685/>.
- Montgomery, D. C. (2017). *Design and analysis of experiments*. John Wiley & Sons.
- Myers, W. R., Yang, W., Ryan, K. J., Bergman, M. S., M. Fisher, E., Soo, J.-C., & Zhuang, Z. (2023). Total outward leakage of half-mask respirators and surgical masks used for source control. *Journal of Occupational and Environmental Hygiene*, 20(12), 610–620. <https://doi.org/10.1080/15459624.2023.2257254>
- Pöhlker, M. L., Krüger, O. O., Förster, J.-D., Berkemeier, T., Elbert, W., Fröhlich-Nowoisky, J., Pöschl, U., Pöhlker, C., Bagheri, G., Bodenschatz, E., Huffman, J. A., Scheithauer, S., & Mikhailov, E. (2021). Respiratory aerosols and droplets in the transmission of infectious diseases. *arXiv*. <https://doi.org/10.48550/arXiv.2103.01188>. No. arXiv:2103.01188).
- Prather, K. A., Marr, L. C., Schooley, R. T., McDiarmid, M. A., Wilson, M. E., & Milton, D. K. (2020). Airborne transmission of SARS-CoV-2. *Science*, 370(6514), 303–304. <https://doi.org/10.1126/science.abf0521>
- Rengasamy, S., Eimer, B., & Shaffer, R. E. (2010). Simple respiratory protection—evaluation of the filtration performance of cloth masks and common fabric materials against 20–1000 nm size particles. *Annals of Occupational Hygiene*. <https://doi.org/10.1093/annhyg/meq044>
- Sall, J., Stephens, M. L., Lehman, A., & Loring, S. (2017). *JMP start statistics: A guide to statistics and data analysis using JMP* (6th ed.). SAS Institute.
- Samet, J. M., Prather, K., Benjamin, G., Lakdawala, S., Lowe, J.-M., Reingold, A., Volckens, J., & Marr, L. C. (2021). Airborne transmission of severe acute respiratory syndrome coronavirus 2 (SARS-CoV-2): What we know. *Clinical Infectious Diseases*, 73(10), 1924–1926. <https://doi.org/10.1093/cid/ciab039>
- Saunders, G. H., Jackson, I. R., & Visram, A. S. (2021). Impacts of face coverings on communication: An indirect impact of COVID-19. *International Journal of Audiology*, 60(7), 495–506. <https://doi.org/10.1080/14992027.2020.1851401>
- Shakya, K. M., Noyes, A., Kallin, R., & Peltier, R. E. (2017). Evaluating the efficacy of cloth facemasks in reducing particulate matter exposure. *Journal of Exposure Science and Environmental Epidemiology*, 27(3), 352–357. <https://doi.org/10.1038/jes.2016.42>
- Tcharkhtchi, A., Abbasnezhad, N., Zarbini Seydani, M., Zirak, N., Farzaneh, S., & Shirinbayan, M. (2021). An overview of filtration efficiency through the masks: Mechanisms of the aerosols penetration. *Bioactive Materials*, 6(1), 106–122. <https://doi.org/10.1016/j.bioactmat.2020.08.002>
- Teasing, G. R., Van Straten, B., De Man, P., & Horeman-Franse, T. (2020). Is there an adequate alternative to commercially manufactured face masks? A comparison of various materials and forms. *Journal of Hospital Infection*, 106(2), 246–253. <https://doi.org/10.1016/j.jhin.2020.07.024>
- Todea, A. M., Schmidt, F., Schuldt, T., & Asbach, C. (2020). Development of a method to determine the fractional deposition efficiency of full-scale HVAC and HEPA filter cassettes for nanoparticles  $\geq 3.5$  nm. *Atmosphere*, 11(11), 1191. <https://doi.org/10.3390/atmos11111191>
- Wang, C. C., Prather, K. A., Sznitman, J., Jimenez, J. L., Lakdawala, S. S., Tufekci, Z., & Marr, L. C. (2021). Airborne transmission of respiratory viruses. *Science*, 373(6558), Article eabd9149. <https://doi.org/10.1126/science.abd9149>
- Yang, W., Myers, W., Bergman, M., Fisher, E., Ryan, K. J., Vollmer, B., Portnoff, L., & Zhuang, Z. (2025a). Total outward leakage of face-worn products used by the general public for source control. *American Journal of Infection Control*, 53(2), 239–244. <https://doi.org/10.1016/j.ajic.2024.09.020>
- Yang, W., Myers, W. R., Bergman, M., Fisher, E., Ryan, K. J., Vollmer, B., Portnoff, L., & Zhuang, Z. (2025b). Evaluating source control efficacy against exhaled submicron particles: Total outward leakage of surgical masks and half facepiece respirators across a spectrum of particle sizes. *Aerosol Science and Technology*, 5(9), 487–498. <https://doi.org/10.1080/02786826.2024.2427282>
- Zangmeister, C. D., Radney, J. G., Vicenzi, E. P., & Weaver, J. L. (2020). Filtration efficiencies of nanoscale aerosol by cloth mask materials used to slow the spread of SARS-CoV-2. *ACS Nano*, 14(7), 9188–9200. <https://doi.org/10.1021/acsnano.0c05025>
- Zhuang, Z., Bradtmiller, B., & Shaffer, R. E. (2007). New respirator fit test panels representing the current U.S. Civilian work force. *Journal of Occupational and Environmental Hygiene*, 4(9), 647–659. <https://doi.org/10.1080/15459620701497538>